




# HEALTH PROTECTION USING CLAY MINERALS: A CASE STUDY BASED ON THE REMOVAL OF BPA AND BPS FROM WATER

GIORA RYTWO<sup>1,2\*</sup> , SHEM LEVY<sup>1</sup>, YUVAL SHAHAR<sup>1</sup>, IDO LOTAN<sup>1</sup>, ARYE LEV ZELKIND<sup>1</sup>, TOMER KLEIN<sup>2</sup>, AND CHEN BARAK<sup>2</sup>

<sup>1</sup>Department of Environmental Sciences and Department of Water Sciences, Tel Hai College, Upper Galilee, Israel 1220800

<sup>2</sup>Environmental Physical Chemistry Laboratory, MIGAL – Galilee Research Institute, Kiryat Shmona, Israel 1101602

**Abstract**—Anthropogenic activity releases hazardous contaminants and pollutants that are not removed fully by water treatments. Among such pollutants, bisphenol-A (BPA) and bisphenol-S (BPS) are included in a series of Endocrine Disruptive Compounds, which may cause disruption due to hormone blockage or mimicking. Thus, even though those pollutants are not considered lethal, they are hazardous to health due to their similarity to 17 $\beta$ -estradiol, and they have been shown to cause developmental malformation in Zebrafish and breast and prostate tumors in rodents. Both BPA and BPS have been found in water sources at concentrations >30  $\mu\text{g L}^{-1}$  and since water treatment plants are ineffective at removing them, their concentration is constantly increasing. The purpose of the present study, using a collection of experiments performed by B.Sc. and M.Sc. students, was to apply clay-based materials to the removal of such health hazards from water. Specifically adapted modified clays as neutral organoclays can optimize the interaction between pollutants and the matrix to achieve efficient adsorption. Such an approach is very effective for relatively insoluble pollutants such as BPA, but less so for the more soluble BPS. On the other hand, BPS can be photodegraded catalytically using raw clay or TiO<sub>2</sub>-impregnated clay. At low catalyst concentration, the modified clay was as effective as a commercial TiO<sub>2</sub> catalyst, whereas combining it with H<sub>2</sub>O<sub>2</sub> yielded considerably better results. In summary, clay minerals offer solutions for the removal of health-hazardous pollutants from water, based on different procedures and mechanisms. The versatility of clay minerals allows 'tailoring' specifically adapted materials that might improve their efficiency based on such very specific pollutant-matrix interactions.

**Keywords**—Adsorption · Bisphenol-A · Bisphenol-S · Clays and health · EDC · Organo-clays · Photocatalysis · TiO<sub>2</sub>-impregnated clay

## Abbreviations

[A] <sub>t</sub>	Relative dimensionless concentration at time <i>t</i>
AOP	Advanced oxidation process
B1	Thiamine (Vitamin B1)
B1-SWy-2	B1 organo-montmorillonite
BPA	Bisphenol-A (4,4'-isopropylidenediphenol)
BPS	Bisphenol-S (4,4'-sulfonylbisphenol)
CMS	The Clay Minerals Society
EDCs	Endocrine Disruptive Compounds
LC-MS/MS	Liquid chromatography tandem-mass spectrometry
<i>k</i> <sub>app</sub>	Apparent rate coefficient
<i>K</i> <sub>L</sub>	Langmuir coefficient
<i>K</i> <sub>p</sub>	Partition coefficient in dual model equation
<i>n</i> <sub>app</sub>	Apparent or "pseudo" reaction order
P25	Commercial high quality catalyst grade TiO <sub>2</sub>
RMSE	Root mean square error

<i>S</i> <sub>max</sub>	Maximum adsorption in Langmuir equation
SYn-1	"Barasym" SSM100 synthetic montmorillonite from the Source Clays Repository of CMS
SWy-2	Wyoming montmorillonite from the Source Clays Repository of CMS
TiO <sub>2</sub> -barasym	Barasym impregnated with TiO <sub>2</sub>
TTIP	Titanium(IV)-isopropoxide
UVC	Light with wavelength 100-280 nm
UV-Vis	UV-visible
XRF	X-ray fluorescence

## INTRODUCTION

Freshwater resources are limited and should not be considered as self-renewable and low-cost (Semiat, 2000). With increasing population, it is obvious that sewage and effluents derived directly or indirectly from anthropogenic sources increase and are not removed fully by conventional water-treatment procedures (Loos et al., 2013). Dissolved organic pollutants, some being highly toxic, carcinogenic, and with long residence times in the environment (El-Shahawi et al., 2010; Unuabonah & Taubert, 2014), e.g. personal care products, hormones, and drug residues ('emerging contaminants'), are recorded in natural streams (Grassi et al., 2012), and may accumulate to biologically hazardous levels (Di Credico et al., 2015).

Among such pollutants, Endocrine Disruptive Compounds (EDCs) from natural or anthropogenic sources (Lintelmann et al., 2003), may cause disruption due to hormone blocking or mimicking, thus interfering with normal hormone activity

This paper belongs to a special issue on 'Clay Minerals in Health Applications.'

**Supplementary Information** The online version contains supplementary material available at <https://doi.org/10.1007/s42860-021-00166-1>.

\* E-mail address of corresponding author: giorarytwo@gmail.com; rytwo@telhai.ac.il

DOI: 10.1007/s42860-021-00166-1

© The Clay Minerals Society 2021

and leading to health problems in organisms and even to their descendants (Bolong et al., 2010).

Two EDCs used widely in industry are bisphenol-A (BPA) and bisphenol-S (BPS) (Fig. 1). BPA (4,4'-isopropylidenediphenol, M.W. 228.3 g mole<sup>-1</sup>) is a chemical used in industry as raw material for the manufacture of polycarbonate, epoxy resins, polyesters, styrenes, etc. (Staples et al., 2000), and it is found in all kinds of plastic pipes, bottles, and food containers (Vandenberg et al., 2007). Its manufacture is projected to reach 7.4 million tons globally by the end of 2023, and is increasing at 3% per year (Research & Markets, 2018). Physiologists consider that BPA is detected incorrectly by cells as estrogen, causing endocrine disruption (Le Fol et al., 2017). Due to the increased awareness of the health hazards posed by BPA, several countries have limited its use since 2011 in food-related accessories, especially in babies' feeding bottles, and the notation "BPA-free" became widely-used. In most cases, however, it was replaced by similarly hazardous BPA analogs such as bisphenol-S (BPS; 4,4'-sulfonylbisphenol, M.W. 242.3 g mole<sup>-1</sup>) or bisphenol-F (BPF; 4,4'-dihydroxydiphenylmethane).

BPS exposure at levels of 60 mg (kg body weight)<sup>-1</sup> day<sup>-1</sup> was found to disrupt endocrine activity (Grignard et al., 2012). Those values are not significantly different from hazardous exposure levels to BPA (50 mg (kg body weight)<sup>-1</sup> day<sup>-1</sup>) (Le Fol et al., 2017). Furthermore, due to the extensive use of BPS in thermal paper, 88% of human exposure has been found to come from receipts and similar uses (Konkel, 2013; Thayer et al., 2016).

In summary, although those pollutants are not considered lethal to humans, they have a hazardous influence due to their similarity to 17 $\beta$ -estradiol (a feminine estrogen hormone). This influence causes, for example, developmental malformation in Zebrafish embryo-larvae at levels as low as 5 and 100 mg L<sup>-1</sup> BPA and BPS, respectively (Moreman et al., 2017; Salahinejad et al., 2020). Additional studies performed on rodents during the last 10 years indicate that BPA, at least, may promote breast and prostate tumors (Seachrist et al., 2016).

Because wastewater treatment plants are only partially effective at removing BPA and BPS (Mohapatra et al., 2011), their concentration in water sources is constantly increasing (Yamazaki et al., 2015), and, in some cases, has reached >30  $\mu$ g L<sup>-1</sup> (Lintelmann et al., 2003). In a mini-review focusing on BPA occurrences, Onundi et al. (2017) concluded that human exposure to them may occur in some cases from drinking water, while other recent studies (Fang et al., 2020) mentioned that BPS concentrations in aqueous environments are increasing constantly, concluding that

"removal from water and its degradation behavior require urgent attention."

Methods for the removal of health-hazardous EDCs from water are based on one or more of the following three approaches: biological degradation (Danzl et al., 2009; Frankowski et al., 2020), adsorption (Bhatnagar & Anastopoulos, 2017; Wirasmita et al., 2018), or advanced oxidation processes (Chen et al., 2006; Mehrabani-Zeinabad et al., 2015). Biological degradation is relatively effective in wastewater treatments plants, with a half-life of 4–5 days (Staples et al., 2000); however, in river waters only 20% degradation was observed, even after 50 days (Frankowski et al., 2020). The latter study also reported that BPS is slightly more biodegradable in river waters but considerably more stable than BPA in wastewaters. Thus, even though bisphenol species are not considered to be 'persistent' from the biodegradation point of view, the amounts of sources and expected hazards are so vast that additional and more effective removal alternatives based on the other two approaches should be considered.

A broad selection of adsorption media – from organic waste and activated carbon to nanocomposites – was tested for bisphenol molecules. However, an extensive review focusing on adsorption matrices for BPA (Bhatnagar & Anastopoulos, 2017) mentioned that "due to the lack of column-, pilot-, and full-scale studies, it is difficult to estimate the potential of these adsorbents in real applications of BPA removal under real environmental conditions." Adsorption matrices based on clays, organo-clays, or nanocomposites for the removal of hazardous pollutants have been used widely and increasingly since the middle of the 20<sup>th</sup> century. The low cost of these materials, their wide availability, and the fact that they are, in most cases, non-toxic make them useful matrices for the adsorption of heavy metals (as raw minerals) as well as organic non-charged or anionic pollutants (upon modifications) (Churchman et al., 2006). Numerous studies of specific sorbents based on clays were reviewed in the course of the present study. In the case of organic non-charged pollutants as BPA and BPS, special attention has been given to the capabilities of organo-clays (Theng et al., 2008). While only a few works reported adsorption of BPS on clay-based materials (Fang et al., 2020), several pillared clays and organo-clays based on quarternary ammonium cations were tested for BPA adsorption (Bhatnagar & Anastopoulos, 2017). Other studies utilized  $\pi$ - $\pi$  interactions between BPA and pyridinium surfactant-based organo-clays (Yang et al., 2016). In the current study, the efficiency of  $\pi$ - $\pi$  interactions was tested along with

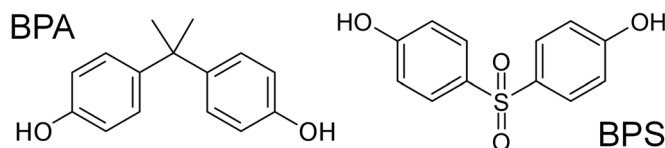


Fig. 1 Schematic structure of BPA (left) and BPS (right)

isotherms and breakthrough columns for the adsorption of BPA and BPS on a food-grade organo-clay based on thiamine (B1 vitamin, consists of an aminopyrimidine aromatic ring bound to a thiazolium ring via  $\text{CH}_2$  group) and montmorillonite. This organo-clay has been found to be very effective for the removal of phenol in aqueous solutions (Ben Moshe & Rytwo, 2018).

In addition to biodegradation and adsorption, a third approach was based on advanced oxidation processes (AOP) that are defined as "water treatment processes performed at pressure and temperature close to environmental conditions, which involve the generation of hydroxyl radicals in sufficient quantity to interact with the organic compounds of the medium" (Cuerda-Correa et al., 2019). AOP processes can be homogeneous (when all components are in the liquid phase) or heterogeneous (when the catalyst is a solid) (Poyatos et al., 2010). Most photodegradation studies on bisphenol compounds were performed with homogeneous catalysis or Fenton-like processes (Fang et al., 2020; Goulart de Araujo et al., 2017; Mehrabani-Zeinabad et al., 2015; Onundi et al., 2017). Heterogeneous photocatalysis was also tested, either with the widely used  $\text{TiO}_2$  or other oxides (Abo et al., 2016; Fang et al., 2020) and even organo-clays (Yang et al., 2016).

Several reaction paths are suggested for the heterogeneous catalysis process; all begin with interaction between photons, the solid catalyst, and the pollutant (Herrmann, 1999; Rytwo, 2018). The most widely available commercial photocatalyst, P25 type  $\text{TiO}_2$  (Schneider et al., 2014), is based on a combination of three phases of  $\text{TiO}_2$ : anatase, rutile, and amorphous (Ohtani et al., 2010), and is considered to be a 'gold standard photocatalyst.' The search for a cheaper/more effective heterogeneous catalysts is ongoing, and several studies have combined clay minerals (Herney-Ramirez et al., 2010; Iurascu et al., 2009; Ramirez et al., 2007), organo-clays, and even  $\text{TiO}_2$ -pillared clays or clays impregnated with  $\text{TiO}_2$  (Bel Hadjtaief et al., 2019; Chen et al., 2013). In the current study the focus was on comparing the basic properties of a synthetic montmorillonite (Syn-1 "Barasym"), either raw or impregnated with  $\text{TiO}_2$ . Additional experiments with the addition of a small amount of  $\text{H}_2\text{O}_2$  ( $2 \text{ mg L}^{-1}$ ,  $58.8 \mu\text{M}$ ) were performed to test a combined heterogeneous/homogeneous process.

Considering the detrimental health effects of BPA and BPS, and their general and increasing importance, the objectives of the current study (carried out by B.Sc. and M.Sc. students) were to measure the adsorption or photodegradation of BPA and BPS in waters using clays, organo-clays, or modified clays. The results indicate that: (a) B1-montmorillonite organo-clay might be relatively effective for the adsorption of BPA but less successful in the case of BPS; and (b) photocatalytic degradation, combining clays (original or modified) with  $\text{H}_2\text{O}_2$ , offers a very fast and effective mineralization process even when applied at low catalyst concentrations. The testing of BPA photocatalysis was beyond the scope of this project due to the formation of degradation byproducts that absorb in the UV-Vis range.

## MATERIALS AND METHODS

### Materials

SWy-2 montmorillonite and SYN-1 Barasym SSM-100 synthetic mica-montmorillonite were obtained from the Source Clays Repository of The Clay Minerals Society. Thiamine hydrochloride (>99%), BPA, BPS, materials for the preparation of  $\text{TiO}_2$ -barasym clay (TTIP, titanium(IV)-isopropoxide 97%), catalyst-grade industrial  $\text{TiO}_2$  (Hombikat®), and a 30% (9.79 M) concentrated  $\text{H}_2\text{O}_2$  solution were obtained from Merck/Sigma-Aldrich (Merck KGaA, Darmstadt, Germany). Sand for the breakthrough columns was collected from the Mediterranean coast in northern Israel. All materials were used without further treatment, except the sand which was sieved for particles >2 mm, and washed four times with distilled water to remove excess salt. All the experiments were performed at ambient conditions ( $23 \pm 2^\circ\text{C}$ ).

### B1-SWy-2 Organo-Clay and $\text{TiO}_2$ -Barasym Preparation

The SWy-2 organo-clay (denoted B1-SWy-2) for the BPA and BPS batch and column adsorption experiments were prepared as described in previous studies (Ben Moshe & Rytwo, 2018): to a homogeneous dispersion of 1 g of SWy-2 with 100 mL distilled water, 175 mg of thiamine powder was added gradually, while stirring. The organo-clay was allowed to reach equilibrium for at least 24 h. The remaining B1 was washed by centrifuging the suspension then replacing 90.0% of the supernatant with distilled water three times, after which no measurable amounts of B1 remained in the supernatant. The final amount of organic cation adsorbed ( $\sim 0.6 \text{ mole kg}^{-1}$ ) was evaluated by measuring thiamine concentration in the supernatants and performing mass balance. The  $\text{TiO}_2$  barasym photocatalyst was prepared by the "impregnation method" (Bel Hadjtaief et al., 2019) by adding, while stirring, 5 g of barasym clay to 20 mL of TTIP solution and heating to  $150^\circ\text{C}$  for 5 h. As in the case of B1-SWy2, the remaining reagents were removed by washing, and the  $\text{TiO}_2$  barasym catalyst was dried at  $105^\circ\text{C}$  for 24 h and calcined at  $500^\circ\text{C}$  in a  $\text{N}_2$  purged vessel for 3 h. To confirm successful impregnation of  $\text{TiO}_2$  on barasym clay, X-ray fluorescence (XRF) measurements (Fig. 2) of the dried powders were made in a He atmosphere at 10, 20, 40, and 50 keV using a S2 Ranger Energy Dispersive XRF (Bruker GmBh, Karlsruhe, Germany). Semiquantitative evaluation of the XRF spectrum, performed using an adapted EQUA-ALL application in *Spectra EDX* v.2.4.2 software program (Bruker GmBh), indicated that while in the raw barasym clay 27% and 22% of the atoms were Si and Al, respectively, and no Ti was measured; in the  $\text{TiO}_2$ -barasym sample only 8.2% and 7.8% of the atoms were Si and Al, respectively, while 39% were Ti atoms. Those results can be observed clearly in Fig. 2.

### Adsorption Isotherms and Column Breakthrough Experiments

BPA and BPS isotherms of raw or B1-SWy-2 montmorillonite were measured, as described in a previous study (Ben Moshe & Rytwo, 2018) in 15-mL plastic tubes with screw caps by adding 1 mL of a stirred  $10 \text{ g L}^{-1}$  of the relevant clay

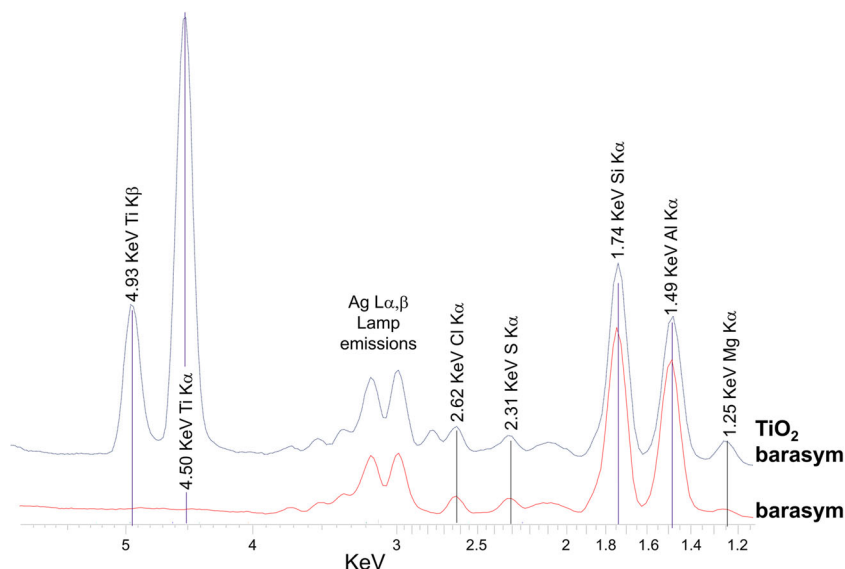


**Fig. 2** XRF spectra of barasym and TiO<sub>2</sub>-barasym irradiated with a 10 KeV Ag lamp

dispersion, and the relevant amounts of BPA or BPS ranging between 0–0.4 mmole adsorbate g<sup>-1</sup> of adsorbent. Distilled water was added to give a final volume of 14 mL. The tubes were agitated on an orbital shaker for 24 h to ensure equilibrium, which was confirmed by measuring again after 48 h. Preliminary studies had shown that the molar absorption coefficient of BPA and BPS at the wavelengths used for determination of the concentration did not change significantly in the range of pH of the experiment (pH ≈ 7.0). From each tube, 1.5 mL was transferred to Eppendorf vials that were then centrifuged at 12,000 rpm (RCF = 9700×g) in a SciLogex D2012 Eppendorf centrifuge (SCIOGEX, Rocky Hill, Connecticut, USA) for 15 min to separate the solids from the supernatant. The concentration of the adsorbate (BPA or BPS) in the supernatant was measured using a diode-array HP 8452A UV-Vis spectrophotometer (Hewlett-Packard Company, Palo Alto, California, USA), and determined by absorbance at 276 nm (OD<sub>276</sub>) for BPA ( $\epsilon = 3060 \text{ M}^{-1} \text{ cm}^{-1}$ ) and OD<sub>260</sub> for BPS ( $\epsilon = 18500 \text{ M}^{-1} \text{ cm}^{-1}$ ), respectively. Experiments were performed in three replications, and average values and standard deviations were calculated. The isotherm results were adapted to a dual mode adsorption model, based on a combination of the Langmuir equation (the left term on the right side) and chemical partition between the adsorbent and the solvent (right term on the right side) (Gonen & Rytwo, 2006).

$$q = \frac{K_L S_{\max} C}{(1 + K_L C)} + K_p C \quad (1)$$

where  $q$  is the amount adsorbed (in mole kg<sup>-1</sup>),  $C$  is the adsorbate equilibrium concentration (M),  $S_{\max}$  is the amount of adsorption sites per mass of adsorbent (mole kg<sup>-1</sup>),  $K_L$  represents the Langmuir adsorption constant (M<sup>-1</sup>), and  $K_p$  is a partitioning coefficient (in L kg<sup>-1</sup>). The relevant coefficients ( $K_L$ ,  $K_p$ , and  $S_{\max}$ ) were evaluated using the 'Solver' algorithm

in Excel® software (Office 365, Microsoft Intl.), to minimize the sum of root mean-squared error (RMSE) between measured and calculated values.

Columns for breakthrough experiments were prepared using plastic tubes with a cross section of 5.59 cm<sup>2</sup> (diameter = 2.67 cm) and a total volume of 40 cm<sup>3</sup>. The tubes were filled with mixtures of sand and clay mineral or organo-clay. The sand was added to avoid clogging and ensure relatively fast flow of the effluent. Control columns contained sand and 1% (w/w) crude SWy-2, while the experiment columns contained sand and 1% B1-SWy-2 organo-clay. BPA and BPS effluents were 0.225 and 0.4 mM, respectively, flowing at a volume rate of  $3.2 \pm 0.02 \text{ mL min}^{-1}$ . BPA and BPS concentrations at the outflow were measured as described above and normalized to the initial concentration ( $C/C_0$ ). The pore volume of columns was measured by the "water-displacement method" (Montes et al., 2005) based on measuring the volume of water needed to fill the pores in a certain volume of medium. Experiments were performed twice.

#### Photocatalysis Experiments

In order to evaluate the efficiency of clay or TiO<sub>2</sub>-clay in photocatalytic degradation of EDCs, several irradiation experiments were performed in a 100-mL UV-C-transparent quartz glass (refractive index  $n = 1.5048$ ), 5.3-cm diameter beaker placed in a Rayonet RMR-600 mini photochemical chamber reactor (Southern New England Ultraviolet Company, Branford, Connecticut, USA), as described in previous studies (Rendel & Rytwo, 2020a, 2020b). The photoreactor was equipped with eight RMR 2537A lamps (254 nm wavelength), each lamp emitting an irradiance flux of  $19 \text{ J m}^{-2} \text{ s}^{-1}$  at 254 nm, as measured in the center of the chamber using a Black Comet SR spectrometer with an F400 UV-VIS-SR-calibrated fiber optic probe equipped with a CR2 cosine light receptor (StellarNet Inc., Tampa, Florida, USA). The same spectrometer was used to measure the spectrum of the solution

with a 20 mm pathlength DP400 dip probe cuvette placed inside the beaker. The solution was mixed constantly with an external stirrer (VELP Scientifica, Usmate Velate, Italy) rotating at 100 rpm. Spectra were measured using the *SpectraWiz* software (StellarNet Inc., Tampa, Florida, USA) every 10–20 s for 30–60 min. Data was transformed to comma separated value (CSV) files, and absorption at the maxima of each chemical (260 or 276) was downloaded after subtracting a baseline value at wavelengths depending on the sample. To allow comparisons between parameters in different reaction mechanisms, the “relative dimensionless concentration at time  $t$ ”  $[A]_{(t)}$  was evaluated (Rytwo et al., 2015) as  $C_t/C_0 = OD_t/OD_0$  (the ratio of actual to initial concentration, or actual to initial light absorbance); thus  $A_0 = 1$ . This procedure led to >200 data points for each experiment.

Considering that all parameters in each experiment remained constant, the rate of photodegradation of BPA or BPS can be defined by a simple rate law (Rendel & Rytwo, 2020a, 2020b):

$$v = \frac{d[A]}{dt} = -k_{\text{app}}[A]^{n_{\text{app}}} \quad (2)$$

where  $v$  is the reaction rate,  $k_{\text{app}}$  is the apparent rate coefficient,  $A$  is the relative dimensionless concentration, and  $n_{\text{app}}$  is the apparent or ‘pseudo’ reaction order.  $n_{\text{app}}$  can be found empirically and is related to the mechanism by which the process occurs. It should be emphasized that high values for  $n_{\text{app}}$  indicate higher degradation rates ( $\frac{d[A]}{dt}$ ) at large concentrations; but, at very low pollutant concentrations, lower orders yield better performance. The term ‘pseudo’ is used to acknowledge the fact that all other influencing parameters (catalyst/degradation agent, temperature, light, etc.) were kept constant (IUPAC, 2014). Because  $A$  is dimensionless, none of the parameters has concentration units. This is convenient because it yields apparent kinetic coefficients that always have dimensions per time, regardless of the order of the process (Rytwo et al., 2015). Analytical integration of Eq. 2 yields:

$$[A]_{(t)} = \left( \frac{1}{\frac{1}{[A_0]^{n_{\text{app}}-1}} + (n_{\text{app}}-1)k_{\text{app}}t} \right)^{\frac{1}{n_{\text{app}}-1}} \quad (3)$$

From the large amount of data in each experiment, a “bootstrap” (Efron, 1979; Mishra et al., 2011) procedure was performed by choosing five sets of 20 random values for each experiment. Values of  $k_{\text{app}}$  and  $n_{\text{app}}$  were calculated by evaluating  $[A]_{(t)}$  using Eq. 3, and finding to each set the best possible parameters using the ‘Solver’ algorithm in *Excel*® software, to minimize the RMSE between measured and calculated  $[A]_{(t)}$  values (Rytwo & Zelkind, 2022). Half-life times were evaluated by solving mathematically Eq. 3 for the case where  $[A]_{(t)} = 0.5$ , yielding

$$t_{1/2} = \frac{2^{n_{\text{app}}-1}-1}{(n_{\text{app}}-1)k_{\text{app}}[A_0]^{n_{\text{app}}-1}} = \frac{2^{n_{\text{app}}-1}-1}{(n_{\text{app}}-1)k_{\text{app}}} \quad (4)$$

The simplification in the right-hand term is, as mentioned above, due to  $A_0 = 1$ . For all three parameters in each experiment ( $k_{\text{app}}$ ,  $n_{\text{app}}$ , and  $t_{1/2}$ ), averages and confidence values at  $\alpha = 0.001$  of the five sets of randomly chosen values were evaluated.

Preliminary experiments were performed to test the accuracy of UV-Vis measurements in the determination of the concentration of BPA and BPS. For this purpose, BPA and BPS photodegradation was tested with no catalysts or reagents (photolysis) by placing in the photoreactor a 25 mg L<sup>-1</sup> concentration of each of the EDCs and comparing measured results from the UV-Visible measurements with an LC-MS/MS analysis performed with a heated electrospray ionization (HESI-II) source connected to a Thermo Scientific™ Q Exactive™ Plus Hybrid Quadrupole-Orbitrap™ Mass Spectrometer (Thermo Fisher Scientific GmbH, Darmstadt, Germany). ESI capillary voltage was set to 3500 V, capillary and gas temperature to 350°C, and gas flow to 35 mL/min. The mass spectra ( $m/z$  50–500) were acquired in negative-ion mode. Peak determination and peak-area integration were performed using Compound Discoverer (*Thermo Xcalibur*, Version 3.1.0.305). The conclusion of this preliminary experiment (see the Results section) was that, while BPS concentration can be determined reliably by UV-Vis measurements, BPA ‘apparent’ concentrations measured by UV-Vis spectroscopy, are erroneous, presumably due to aromatic degradation products that absorb light strongly at the wavelength used.

Based on the preliminary results, the following experiments with an initial BPS concentration of 5 mg L<sup>-1</sup> (20.6 μM) BPS were performed: (a) photolysis (photodegradation with no catalyst); (b) photocatalysis using the ‘gold standard’ P-25 TiO<sub>2</sub> photocatalyst; (c) photocatalysis using barasym synthetic montmorillonite; (d) photocatalysis using TiO<sub>2</sub>-barasym prepared as described in the B1-SWy-2 *Organo-clay and TiO<sub>2</sub>-barasym preparation* subsection; (e) as (a) with the addition of a low concentration (58.8 μM) of H<sub>2</sub>O<sub>2</sub>; (f) as (c) with 58.8 μM H<sub>2</sub>O<sub>2</sub>; and (g) as (d) with 58.8 μM H<sub>2</sub>O<sub>2</sub>. The last three experiments were performed to test the contribution of an auxiliary component in order to perform a combination of “photo-Fenton process” (Poyatos et al., 2010) with heterogeneous catalysis. In all the experiments, catalyst concentration was 20 mg L<sup>-1</sup>. After analyzing the results, a second set of experiments was performed, identical to (b)–(d), (f), and (g), but the concentrations of catalysts (barasym, TiO<sub>2</sub>-barasym, and TiO<sub>2</sub>) were reduced by two orders of magnitude to 0.2 mg L<sup>-1</sup>.

## RESULTS AND DISCUSSION

### Adsorption Isotherms

The adsorption isotherms of BPA and BPS to B1-SWy-2 *organo-clay* are shown in Fig. 3. Adsorption to raw SWy-2 is

not shown; preliminary experiments indicated that it was null. As reported and reviewed extensively, organophilic matrices adsorb hydrophobic organic compounds efficiently (Churchman et al., 2006; Nafees & Waseem, 2014), and have been used in water treatment. Indeed, the organophilic modification with B1 converted the montmorillonite (that did not adsorb BPA and BPS at all) to a relatively efficient removal matrix.

The adsorption results of BPA fit the dual model very well, but do not fit the regular Langmuir equation as well and do not reach a real saturation value in the range tested. On the other hand, adsorption of BPS fits the Langmuir model very well, giving a saturation value of  $\sim 0.13$  mole  $\text{Kg}^{-1}$ . The improvement obtained using the dual model for BPS is not very significant, and this is supported by the fact that the partition coefficient is about one order of magnitude lower than for BPA (see Table 1). The noticeable difference in the isotherms is ascribed to the fact that BPS is more hydrophilic than BPA; the solubility of BPS in water is almost four times that of BPA (Samineni, 2017), thus almost no partition effect was observed. For the case of BPA, due to its greater hydrophobicity, very high affinity (H-type) allowing complete removal was observed at low concentrations, whereas partition behavior (C-type) allowed a large capacity for adsorption at larger concentrations, offering it as a relatively effective adsorbent. Phenol-calculated adsorption parameters for the equations based on previous studies (Ben Moshe & Rytwo, 2018) were also added to Table 1 and brought an interesting perspective: partition coefficients for phenol and BPA are similar, whereas  $S_{\text{max}}$  of phenol in the Langmuir equation is almost five times that of BPA and eight times that of BPS. On the other hand, the  $K_L$  value of phenol is relatively low, but this does not hinder the vast adsorption of this pollutant due to the large  $S_{\text{max}}$  according to both models.

### Breakthrough Column Experiments

To complete the picture of the efficiency of B1-SWy-2 in the removal of BPA and BPS from water, column breakthrough flowing experiments were performed. Clay-based materials have very low hydraulic conductivity, thus the flow rate through an organo-clay column is very low (Rytwo, 2018). In 'real' systems, this severe limitation might be solved by using flow-through active slurry filters (Rytwo & Daskal, 2016) or a series of consecutive slurry vessels (Rytwo et al., 2007). However, for laboratory purposes, such a handicap is usually bypassed by mixing the active ingredient (the organo-clay) with inactive sand, quartz, or other materials with good hydraulic properties (Radian et al., 2011). The relative concentration of BPA or BPS in the outflow, as a function of the number of pore volumes of polluted solution introduced to the column, is shown in Fig. 4. For adsorption on organoclay columns, both replicates for each EDC are shown.

Almost no removal of either pollutant occurred in the raw-clay/sand columns, and after 1 pore volume the relative concentration increased, reaching a maximum concentration after 5 and 9 pore volumes for BPA or BPS, respectively (it should be emphasized that the initial concentration of BPS was almost 80% larger than that of BPA).

As for the organo-clay/sand columns in previous studies using the same matrix of a 2% organo-clay/sand, phenol was removed completely from a 0.45 mM solution with >80 pore volumes (Ben Moshe & Rytwo, 2018), whereas complete removal of BPA required just 14 pore volumes. Comparing these two cases is difficult, however, due to differences in pollutant and organo-clay concentrations, but it is obvious that removal of BPA by B1-SWy-2 is considerably less effective than removal of phenol. Such differences can be ascribed to the data shown in the isotherms and in Table 1; the maximum adsorption of BPA was considerably lower than for phenol.

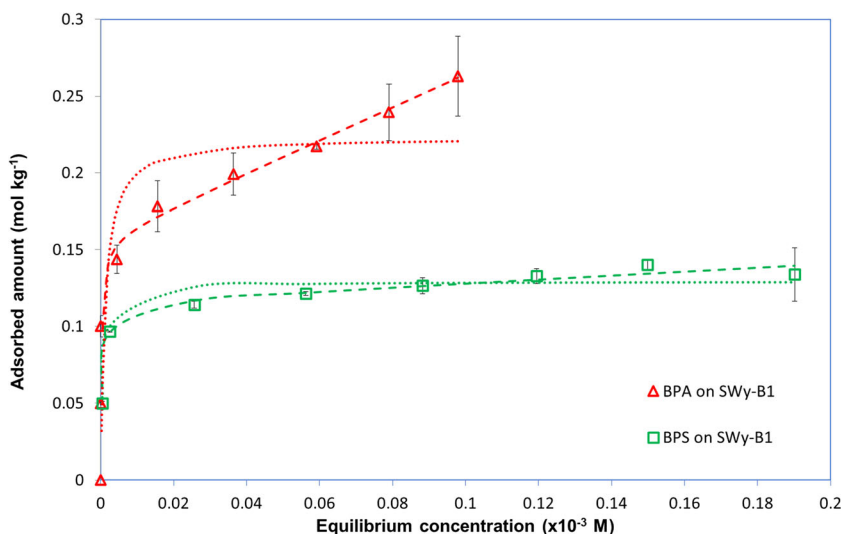


**Fig. 3** Adsorption isotherms of BPA (red triangles and lines) and BPS (green squares and lines). Triangles and squares represent measured values with their respective standard deviations. The lines represent calculations according to the Langmuir equation (dotted lines), or to the dual mode model (dashed lines). Coefficients and fitting parameters are reported in Table 1

**Table 1** Parameters for the calculations of BPA, BPS, and phenol adsorption on B1-SWy-2 organo-clay, according to the Langmuir equation and the dual mode model. Adsorption of phenol was evaluated based on the work of Ben Moshe and Rytwo (2018).

Model	Parameter	BPA	BPS	Phenol
Langmuir equation	$K_L$ (mole $\text{kg}^{-1}$ )	837.3	1373	23.82
	$S_{\text{max}}$ (mole $\text{kg}^{-1}$ )	0.2230	0.1290	1.0500
	$R^2$	0.7336	0.9374	0.9324
	RMSE ( $\mu\text{mole kg}^{-1}$ )	788.2	48.00	7769
Dual mode model	$K_L$ (mole $\text{kg}^{-1}$ )	3278	1902	97.12
	$S_{\text{max}}$ (mole $\text{kg}^{-1}$ )	0.1580	0.1160	0.5797
	$K_p$ (L $\text{kg}^{-1}$ )	1.0681	0.1262	1.1341
	$R^2$	0.9921	0.9867	0.9958
	RMSE ( $\mu\text{mole kg}^{-1}$ )	21.51	10.02	403.69

In the case of BPS removal, the results revealed that removal by the clay/sand column was even less effective than for BPA; pollutant leaks appeared in the outflow after only three pore volumes. Such results might be explained by the combination of low maximum adsorption capacity and no partition effect, as shown in the adsorption isotherms. After breakthrough, however, the behaviors of the two EDCs were completely different. Breakthrough of BPA occurred (as mentioned above) after 14 pore volumes and the increase in outflow concentration was sharp, from no BPA in the outflow, to  $0.8 C_0$  in less than three additional pore volumes, with complete saturation reached after 20 pore volumes. For BPS, the increase after breakthrough was slow and gradual, from  $0.1 C_0$  after  $\sim 3$  pore volumes to up to  $0.8 C_0$  after 20 pore volumes. Similar behavior was reported in previous studies with humic-acid removal by columns based on ODTMA organo-clays (Beall, 2003).

#### Photocatalytic Degradation

As mentioned in the Photocatalysis Experiments subsection, a preliminary experiment was performed to ensure that UV-Vis measurements gave reliable information about the

concentration of BPA and BPS. Photolysis experiments with no catalyst (only UVC light) were performed and concentrations as a function of time were measured by both LCMS/MS and UV-Vis, as described in the Methods section (Fig. 5). While BPS concentrations using both methods were similar, indicating that for BPS UV-Vis may offer a very fast and relatively accurate quantification, the values measured for BPA by the two methods gave completely different results. Detailed LCMS/MS measurements screening the range of molecular weights between 50 and  $500 \text{ g mole}^{-1}$  indicated that indeed there are several aromatic photodegradation byproducts that may be wrongly misinterpreted in a simple UV-Vis evaluation as BPA. Because the study focused on collecting large amounts of data for each experiment (which cannot be done in LCMS/MS measurements), only BPS was tested in subsequent experiments.

The intention of the following experiments was to determine if clay or  $\text{TiO}_2$ -modified clay can act as an effective photocatalyst for BPS. In a review on AOPs for the removal of BPS, a series of studies was reported but in all of them the half-life of BPS was 40–120 min (Fang et al., 2020).

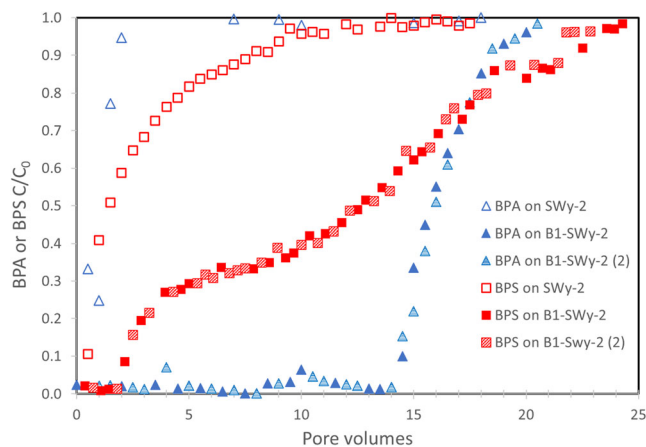


**Fig. 4** Breakthrough curve of a BPA (triangles) or a BPS (squares) solution filtered through sand mixed with 1% B1-SWy-2 organoclay (full or partially full symbols) or sand mixed with 1% raw SWy-2 montmorillonite (empty symbols) columns. Full or partial symbols indicate results from two separate experiments

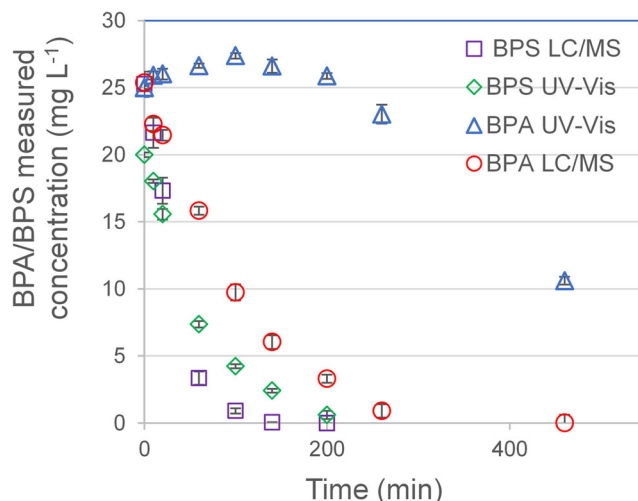


**Fig. 5** Comparison of concentrations measured by LCMS and UV-Vis of the photolytic degradation of BPA and BPS as a function time. The initial concentration of both pollutants was  $25 \text{ mg L}^{-1}$

Heterogeneous photocatalysis with  $\text{TiO}_2$  (Abo et al., 2016) or organo-clays (Yang et al., 2016) gave similar values. Homogeneous photocatalysis ranged between a few minutes (Goulart de Araujo et al., 2020; Mehrabani-Zeinabad et al., 2015) to several tens of minutes (Mehrabani-Zeinabad et al., 2015; Onundi et al., 2017), but short half-life times were observed only at very high concentrations of  $\text{H}_2\text{O}_2$  ( $>3 \text{ mM}$ , 50 times greater than the concentration used in the present study) or combinations of  $\text{H}_2\text{O}_2$  with ozone.

The efficiency of barasym clay or  $\text{TiO}_2$ -barasym clay as a photocatalyst was evaluated based on the half-life ( $t_{1/2}$ ) of the degradation, as compared with photolysis, or a 'gold standard' well known photocatalyst – commercial type P-25  $\text{TiO}_2$  (Rioja et al., 2016). The catalyst concentration was set at  $20 \text{ mg L}^{-1}$  based on previous studies on the photodegradation of carbamazepine (Klein & Rytwo, 2014, unpublished results) which showed that the optimal efficiency was observed at  $<100 \text{ mg L}^{-1}$   $\text{TiO}_2$ . The determination of  $t_{1/2}$  was based (as described in the Methods section) on performing more than 200 UV-Vis measurements for each experiment, and analyzing the change of concentration with time, finding suitable specific  $k_{\text{app}}$  and  $n_{\text{app}}$  values for each case that fitted the integrated simple rate law (Eq. 2).

Figure 6 shows the concentration of BPS as a function of time for the various treatments (a–f in the Photocatalysis Experiments subsection), whereas Fig. 7 summarizes  $t_{1/2}$  and  $n_{\text{app}}$  (the pseudo order) of all the experiments, according to Eqs 2–4. The photolysis process (without catalysts) followed a close to 1<sup>st</sup> order process ( $n_{\text{app}} = 1.02 \pm 0.06$ ), and  $t_{1/2} = 22.0 \pm 0.77 \text{ min}$ . Performing homogeneous photocatalysis with hydrogen peroxide ( $2 \text{ mg L}^{-1} = 58.8 \text{ } \mu\text{M H}_2\text{O}_2$ ) changed the pseudo order of the process to  $n_{\text{app}} = 0.82 \pm 0.03$ , and reduced the half-life time to almost 50% of the value measured by photolysis ( $t_{1/2} = 11.2 \pm 0.07 \text{ min}$ ). The use of clay-based materials as heterogeneous catalysts yielded slightly longer half-life times ( $t_{1/2} = 13.7 \pm 0.12$  and  $13.6 \pm 0.18 \text{ min}$  for barasym and  $\text{TiO}_2$ -barasym, respectively). However, even

though the half-life time for both catalysts was almost the same, the pseudo order was completely different. While for the raw barasym it was almost a pseudo first-order process ( $n_{\text{app}} = 0.95 \pm 0.02$ ), for the  $\text{TiO}_2$ -barasym it was  $n_{\text{app}} = 0.74 \pm 0.04$ . The outcome of it is that the behavior was almost identical for both catalysts at the beginning of the process; but after 15–20 min, differences appeared (Fig. 6) and the  $\text{TiO}_2$ -barasym exhibited slightly better degradation performance at very low concentrations, as expected due to the lower pseudo order of the process (see Eq. 1) (Rytwo & Zelkind, 2022). Thus, the results indicated that clay-based catalysts under current conditions reduce the half-life times to ~55% of photolysis values, reaching results like those obtained by homogeneous catalysis with hydrogen peroxide. An additional observation was that the modification of the clay mineral with  $\text{TiO}_2$  impregnation indeed changes the process in some way, as can be seen by the different pseudo order.

To compare the efficacy of clay-based catalysts with catalysts used commonly, the same experiment was performed using the same concentration of commercial catalyst P25 type  $\text{TiO}_2$ . As mentioned above, this material is considered the 'gold standard' of heterogeneous catalysts, and, indeed, exhibits the best results for this set. While the pseudo order with P25 type  $\text{TiO}_2$  was similar to that of  $\text{TiO}_2$ -barasym ( $n_{\text{app}} = 0.75 \pm 0.05$ ), the half-life time was only 30% of the photolysis value ( $t_{1/2} = 6.8 \pm 0.11 \text{ min}$ ).

Following these results, a test for a possible synergistic effect by combining a "photo-Fenton process" (addition of  $\text{H}_2\text{O}_2$ ) with heterogeneous catalysis using clay-based materials was performed. Results were indeed improved. In barasym/ $\text{H}_2\text{O}_2$ , pseudo order changed to  $n_{\text{app}} = 0.74 \pm 0.06$  and  $t_{1/2} = 8.5 \pm 0.26 \text{ min}$  (62% of the value without hydrogen peroxide). In  $\text{TiO}_2$ -barasym, the pseudo order remained as before ( $n_{\text{app}} = 0.72 \pm 0.05$ ), but the improvement was even more significant (55%,  $t_{1/2} = 7.5 \pm 0.13 \text{ min}$ ), reaching values close to those of the 'gold standard' commercial  $\text{TiO}_2$ .



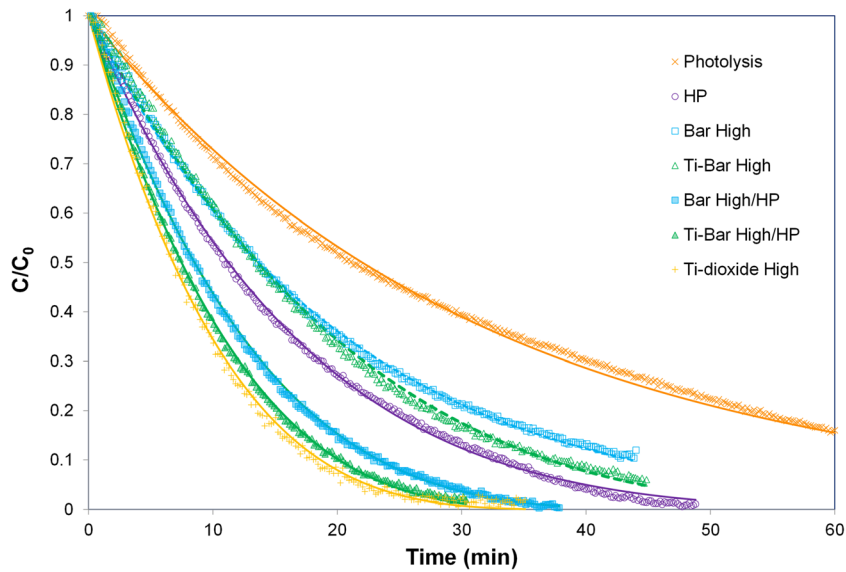


**Fig. 6** Relative concentration in a photodegradation experiment of an initial concentration of  $5 \text{ mg L}^{-1}$  ( $20.6 \text{ } \mu\text{M}$ ) BPS. 'Photolysis' represents the process without catalyst; HP,  $2 \text{ mg L}^{-1} \text{ H}_2\text{O}_2$ ; Bar High, barasym  $20 \text{ mg L}^{-1}$ ; Ti-Bar High,  $\text{TiO}_2$ -barasym  $20 \text{ mg L}^{-1}$ ; Ti-dioxide High, commercial  $\text{TiO}_2$   $20 \text{ mg L}^{-1}$ ; Bar High/HP, barasym  $20 \text{ mg L}^{-1} + 2 \text{ mg L}^{-1} \text{ H}_2\text{O}_2$ ; Ti-Bar High/HP,  $\text{TiO}_2$ -barasym  $20 \text{ mg L}^{-1} + 2 \text{ mg L}^{-1} \text{ H}_2\text{O}_2$

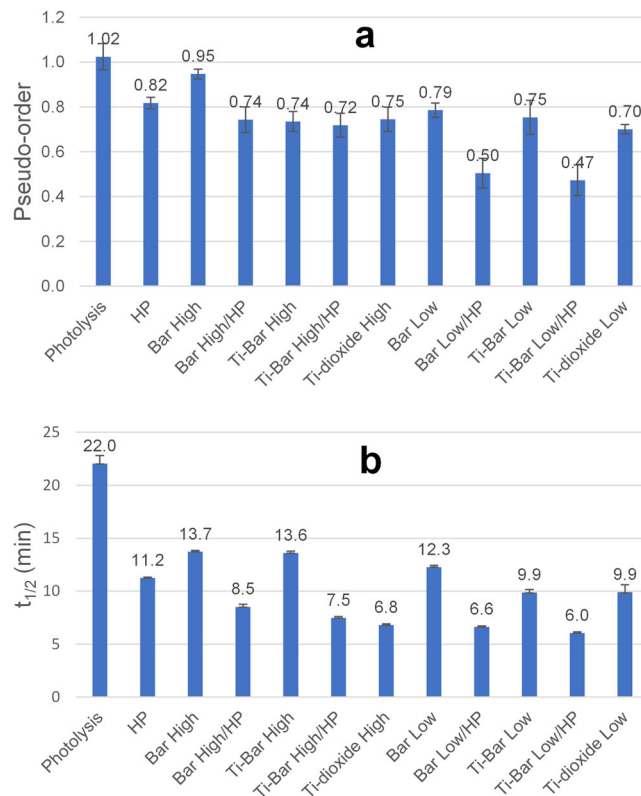


**Fig. 7 a** Pseudo order and **b**half-life time in photodegradation experiments of an initial concentration of  $5 \text{ mg L}^{-1}$  ( $20.6 \text{ } \mu\text{M}$ ) BPS. 'Photolysis' represents the process without catalyst, whereas the term 'HP' indicates  $2 \text{ mg L}^{-1} \text{ H}_2\text{O}_2$ . The terms 'Bar', 'Ti-Bar', and 'Ti-dioxide' indicate barasym,  $\text{TiO}_2$ -barasym, and commercial  $\text{TiO}_2$ , respectively. The terms 'High' and 'Low' indicate catalyst concentration of  $20 \text{ mg L}^{-1}$  or  $0.2 \text{ mg L}^{-1}$ , respectively

Previous studies on caffeine photodegradation (Rendel & Rytwo, 2020a, 2020b) demonstrated high efficiency at TiO<sub>2</sub> concentrations of 1 mg L<sup>-1</sup> and even less. Thus, following the results described above, the photodegradation experiments were performed again, with the same EDC (5 mg L<sup>-1</sup> BPS) and homogeneous catalyst (2 mg L<sup>-1</sup> H<sub>2</sub>O<sub>2</sub>) concentrations, but reducing the heterogeneous catalyst (barasym, TiO<sub>2</sub>-barasym or commercial TiO<sub>2</sub>) by two orders of magnitude to 0.2 mg L<sup>-1</sup>. As mentioned above, Fig. 7 summarizes  $t_{1/2}$  and  $n_{app}$  (the pseudo order) of all the experiments, according to Eqs 2–4. Raw barasym at low catalyst concentration yielded a slightly lower half-life time than at high concentration ( $t_{1/2} = 12.3 \pm 0.16$  instead of  $13.7 \pm 0.12$  min) but the pseudo-order change from almost pseudo first order to  $n_{app} = 0.79 \pm 0.03$ . TiO<sub>2</sub> barasym at 0.2 mg L<sup>-1</sup> appeared to be considerably more effective than at 20 mg L<sup>-1</sup> ( $t_{1/2} = 9.9 \pm 0.29$  instead of  $13.6 \pm 0.18$  min), but with almost identical pseudo order ( $n_{app} = 0.75 \pm 0.08$ ). Decreased efficiency at higher catalyst concentrations was ascribed in previous studies to light dispersion by the colloidal catalysts, and even catalyst aggregation, causing a reduction in the active surface (Chong et al., 2010). In commercial TiO<sub>2</sub> the effect was completely different; reducing the catalyst concentration lowered the efficiency and increased the half-life time ( $t_{1/2} = 9.9 \pm 0.18$  instead of  $6.8 \pm 0.12$  min) with slightly lower pseudo order ( $n_{app} = 0.70 \pm 0.09$  instead of  $0.74 \pm 0.04$ ). The outcome was that while at 20 mg L<sup>-1</sup> catalysts concentration the commercial TiO<sub>2</sub> exhibited better performance than TiO<sub>2</sub>-barasym, the results were almost identical when the catalyst concentration was 0.2 mg L<sup>-1</sup>, thus the modified clay met the 'gold standard' of photocatalysis, under the same conditions.

The most impressive effect was obtained, however, by combining small concentrations of clay-based catalyst with H<sub>2</sub>O<sub>2</sub> (Fig. 7, Fig. S1 in Supplemental Information). In barasym, the parameters changed to  $t_{1/2} = 6.6 \pm 0.09$  min,  $n_{app} = 0.50 \pm 0.07$ , while in TiO<sub>2</sub>-barasym results were even better ( $t_{1/2} = 6.0 \pm 0.11$  min,  $n_{app} = 0.47 \pm 0.07$ ). Thus, both raw clay and TiO<sub>2</sub>-impregnated clay exhibited very good performance at low concentrations, especially in combination with hydrogen peroxide.

As mentioned above (Rytwo & Zelkind, 2022), according to Eq. 1, at low pollutant concentrations processes benefit from lower pseudo orders. From Fig. 7a it can be hypothesized that the real orders that depend on the exact and specific set of "consecutive elementary reactions" (Atkins & de Paula, 2006) are essentially 1, 0.75, or 0.5. Forcing the pseudo order to such rounded values (the best fit between 1, 0.75, or 0.5) delivered almost the same  $t_{1/2}$  in all cases, while  $k_{app}$  changed slightly accordingly. For example, by fixing the pseudo order of the low concentration of TiO<sub>2</sub> to  $n_{app} = 0.75$  instead of the optimized value of 0.70, yielded  $t_{1/2} = 9.7$  min instead of 9.9 min. In all other cases, differences were even smaller. The hypothesis is that a relationship exists between the pseudo order and the efficacy of the process: With less effective processes ( $t_{1/2} > 14$  min) the observed pseudo orders were close to one. When efficacy improved ( $7 \text{ min} < t_{1/2} < 13 \text{ min}$ ), pseudo order was reduced to 0.75. Borderline cases ( $t_{1/2} \approx 13.5 \text{ min}$ ) can be

either one pseudo order or the other (high concentration of barasym is pseudo order  $\approx 1$  whereas high TiO<sub>2</sub>-barasym is  $\approx 0.75$ ). Additional improvement in efficiency ( $t_{1/2} < 7 \text{ min}$ ) was accompanied by reduction of the pseudo order to 0.5.

## SUMMARY

As mentioned in the introduction, bisphenol compounds are considered to be very hazardous. In the pursuit of ways to remove such health concerns from water, this study presented test cases of the use of clay-based materials either as adsorbents or as catalysts.

Results show that bisphenol molecules are not adsorbed on raw clays, but the preparation of organophilic organo-clays can offer a possible effective sorbent, especially for BPA which is more hydrophobic. Adsorption columns combining 1% organo-clay as an active ingredient were able to remove BPA completely for  $\sim 15$  pore volumes. Preparing mixed columns with other active components (such as activated carbon) may improve considerably the efficiency, even though this should be tested in a closer-to-nature environment that includes lower EDC concentrations, and other chemicals that may compete with BPA for adsorption. It is interesting to note that there does not appear to exist a single solution; even though BPA and BPS are considered 'homologue molecules,' the specific matrix used in the present study (B1-SWy-2 organo-clay) exhibited relatively high removal efficiency for BPA but was not very effective at removing BPS, probably due to its relatively high hydrophilicity, leading to the lack of a partition mechanism. More research is required to find specifically adapted adsorbing matrices to optimize the specific interaction with a particular hazardous pollutant case, and a combination of matrices may be required in real cases.

On the other hand, the present study showed that BPS can be removed effectively by photocatalytic processes, using clays or modified clays as catalysts. Based on the results of this test case, another conclusion is that, at low catalyst concentration (0.2 mg L<sup>-1</sup>), clay-based catalysts may be as effective for the photodegradation of BPS as the 'gold standard' P-25 type TiO<sub>2</sub>, especially when combined with low concentrations (0.059 mM) of hydrogen peroxide. Modifications of the clay, such as impregnation with TiO<sub>2</sub>, may yield even better results. Optimization of the process requires additional experimental work because other solution components should also be considered, and their contribution to the photocatalytic process cannot always be predicted. On one hand, BPA homogeneous photocatalysis was severely hindered in wastewater compared with clean water (Goulart de Araujo et al., 2020). On the other hand, while bromide hindered caffeine homogeneous photocatalysis even at very low concentrations, chloride improved the photodegradation when present up to 100 mM but hindered the process at higher concentrations (Rendel & Rytwo, 2020a).

In summary, clay minerals offer solutions for the removal of health-hazardous pollutants from water, based on completely different procedures and mechanisms. The versatility of clay minerals allows us to 'tailor' specifically adapted materials that

might improve their efficiency based on specific pollutant-matrix interactions.

#### ACKNOWLEDGMENTS

The authors thank Prof. Soliman Khatib and the whole team at the Research Laboratory of Tel Hai College for their support with LC-MS/MS measurements, and all the staff at the Hydrogeochemistry Lab at MIGAL Research Institute (headed by Prof. M. Iggy Litaor) for kindly hosting the authors and their photodegradation device at their premises.

#### Funding

Funding sources are as stated in the Acknowledgments.

#### Declarations

#### Conflict of Interest

The authors declare that they have no conflict of interest.

#### REFERENCES

- Abo, R., Kummer, N.-A., & Merkel, B. J. (2016). Optimized photodegradation of Bisphenol A in water using ZnO, TiO<sub>2</sub> and SnO<sub>2</sub> photocatalysts under UV radiation as a decontamination procedure. *Drinking Water Engineering and Science*, 9(2), 27–35. <https://doi.org/10.5194/dwes-9-27-2016>
- Atkins, P., & de Paula, J. (2006). *Physical Chemistry* (Vol. 8th). W.H.Freemans and Co.
- Beall, G. W. (2003). The use of organo-clays in water treatment. *Applied Clay Science*, 24(1–2), 11–20. <https://doi.org/10.1016/j.clay.2003.07.006>
- Bel Hadjltaief, H., Galvez, M. E., Ben Zina, M., & Da Costa, P. (2019). TiO<sub>2</sub>/clay as a heterogeneous catalyst in photocatalytic/ photochemical oxidation of anionic reactive blue 19. *Arabian Journal of Chemistry*, 12(7), 1454–1462. <https://doi.org/10.1016/J.ARABJC.2014.11.006>
- Ben Moshe, S., & Rytwo, G. (2018). Thiamine-based organoclay for phenol removal from water. *Applied Clay Science*, 155, 50–56. <https://doi.org/10.1016/j.clay.2018.01.003>
- Bhatnagar, A., & Anastopoulos, I. (2017). Adsorptive removal of bisphenol A (BPA) from aqueous solution: A review. *Chemosphere*, 168, 885–902. <https://doi.org/10.1016/J.CHEMOSPHERE.2016.10.121>
- Bolong, N., Ismail, A. F., Salim, M. R., Rana, D., Matsuura, T., & Tabe-Mohammadi, A. (2010). Negatively charged polyethersulfone hollow fiber nanofiltration membrane for the removal of bisphenol A from wastewater. *Separation and Purification Technology*, 73(2), 92–99. <https://doi.org/10.1016/j.seppur.2010.01.001>
- Chen, D., Du, G., Zhu, Q., & Zhou, F. (2013). Synthesis and characterization of TiO<sub>2</sub> pillared montmorillonites: Application for methylene blue degradation. *Journal of Colloid and Interface Science*, 409, 151–157. <https://doi.org/10.1016/j.jcis.2013.07.049>
- Chen, P.-J., Linden, K. G., Hinton, D. E., Kashiwada, S., Rosenfeldt, E. J., & Kullman, S. W. (2006). Biological assessment of bisphenol A degradation in water following direct photolysis and UV advanced oxidation. *Chemosphere*, 65(7), 1094–1102. <https://doi.org/10.1016/J.CHEMOSPHERE.2006.04.048>
- Chong, M. N., Jin, B., Chow, C. W. K., & Saint, C. (2010). Recent developments in photocatalytic water treatment technology: A review. *Water Research*, 44(10), 2997–3027. <https://doi.org/10.1016/j.watres.2010.02.039>
- Churchman, G. J., Gates, W. P., Theng, B. K. G., & Yuan, G. (2006). Chapter 11.1: Clays and clay minerals for pollution control. In: F. Bergaya, B. K. G. Theng, G. Lagaly (Ed.), *Developments in Clay Science: Volume 1* (Issue C, pp. 625–675). Elsevier. [https://doi.org/10.1016/S1572-4352\(05\)01020-2](https://doi.org/10.1016/S1572-4352(05)01020-2)
- Cuerda-Correa, E. M., Alexandre-Franco, M. F., & Fernández-González, C. (2019). Advanced oxidation processes for the removal of antibiotics from water. An Overview. *Water*, 12(1), 102. <https://doi.org/10.3390/w12010102>
- Danzl, E., Sei, K., Soda, S., Ike, M., & Fujita, M. (2009). Biodegradation of bisphenol A, bisphenol F and bisphenol S in seawater. *International Journal of Environmental Research and Public Health*, 6(4), 1472–1484. <https://doi.org/10.3390/ijerph6041472>
- Di Credico, B., Bellobono, I. R., D'Arienzo, M., Fumagalli, D., Redaelli, M., Scotti, R., Morazzoni, F., Di Credico, B., Bellobono, I. R., Arienzo, M. D., Fumagalli, D., Redaelli, M., Scotti, R., & Morazzoni, F. (2015). Efficacy of the reactive oxygen species generated by immobilized TiO<sub>2</sub> in the photocatalytic degradation of diclofenac. *International Journal of Photoenergy*, 2015, 1–13. <https://doi.org/10.1155/2015/919217>
- Efron, B. (1979). Bootstrap Methods: Another Look at the Jackknife. *The Annals of Statistics*, 7(1), 1–26. <https://doi.org/10.1214/aos/1176344552>
- El-Shahawi, M. S., Hamza, A., Bashammakh, A. S., & Al-Saggaf, W. T. (2010). An overview on the accumulation, distribution, transformations, toxicity and analytical methods for the monitoring of persistent organic pollutants. *Talanta*, 80(5), 1587–1597. <https://doi.org/10.1016/j.talanta.2009.09.055>
- Fang, Z., Gao, Y., Wu, X., Xu, X., Sarmah, A. K., Bolan, N., Gao, B., Shaheen, S. M., Rinklebe, J., Ok, Y. S., Xu, S., & Wang, H. (2020). A critical review on remediation of bisphenol S (BPS) contaminated water: Efficacy and mechanisms. *Critical Reviews in Environmental Science and Technology*, 50(5), 476–522. <https://doi.org/10.1080/10643389.2019.1629802>
- Frankowski, R., Zgoła-Grzeškowiak, A., Smulek, W., & Grzeškowiak, T. (2020). Removal of Bisphenol A and Its Potential Substitutes by Biodegradation. *Applied Biochemistry and Biotechnology*, 191(3), 1100–1110. <https://doi.org/10.1007/s12010-020-03247-4>
- Gonen, Y., & Rytwo, G. (2006). Using the dual-mode model to describe adsorption of organic pollutants onto an organoclay. *Journal of Colloid and Interface Science*, 299(1), 95–101. <https://doi.org/10.1016/j.jcis.2006.01.055>
- Goulart de Araujo, L., da Silva Santos, F., & Teixeira, A. C. S. C. (2017). Degradation of bisphenol A by the UV and UV/H<sub>2</sub>O<sub>2</sub> processes: Evaluation of process variables through experimental design. *Canadian Journal of Chemical Engineering*, 95(12), 2278–2285. <https://doi.org/10.1002/cjce.22997>
- Goulart de Araujo, L., Oscar Conte, L., Violeta Schenone, A., Alfano, O. M., & Teixeira, A. C. S. C. (2020). Degradation of bisphenol A by the UV/H<sub>2</sub>O<sub>2</sub> process: a kinetic study. *Environmental Science and Pollution Research*, 27(7), 7299–7308. <https://doi.org/10.1007/s11356-019-07361-7>
- Grassi, M., Kaykioglu, G., Belgiomo, V., & Lofrano, G. (2012). *Removal of Emerging Contaminants from Water and Wastewater by Adsorption Process*. Springer Netherlands. [https://doi.org/10.1007/978-94-007-3916-1\\_2](https://doi.org/10.1007/978-94-007-3916-1_2)
- Grignard, E., Lapenna, S., & Bremer, S. (2012). Weak estrogenic transcriptional activities of Bisphenol A and Bisphenol S. *Toxicology In Vitro*, 26(5), 727–731. <https://doi.org/10.1016/j.tiv.2012.03.013>
- Herney-Ramirez, J., Vicente, M. A., & Madeira, L. M. (2010). Heterogeneous photo-Fenton oxidation with pillared clay-based catalysts for wastewater treatment: A review. *Applied Catalysis B: Environmental*, 98(1–2), 10–26. <https://doi.org/10.1016/j.apcatb.2010.05.004>
- Herrmann, J.-M. (1999). Heterogeneous photocatalysis: fundamentals and applications to the removal of various types of aqueous

- pollutants. *Catalysis Today*, 53(1), 115–129. [https://doi.org/10.1016/S0920-5861\(99\)00107-8](https://doi.org/10.1016/S0920-5861(99)00107-8)
- IUPAC. (2014). Compendium of Chemical Terminology: Gold Book. *IUPAC Compendium of Chemical Terminology*, 1670. <https://doi.org/10.1351/goldbook>
- Iurascu, B., Siminicéanu, I., Vione, D., Vicente, M. A., & Gil, A. (2009). Phenol degradation in water through a heterogeneous photo-Fenton process catalyzed by Fe-treated laponite. *Water Research*, 43(5), 1313–1322. <https://doi.org/10.1016/j.watres.2008.12.032>
- Klein, T., & Rytwo, G. (2014). *B.Sc. internal project*. Environmental Sciences Dept., Tel Hai College.
- Konkel, L. (2013). Thermal Reaction: The Spread of Bisphenol S via Paper Products. *Environmental Health Perspectives*, 121(3). <https://doi.org/10.1289/ehp.121-a76>
- Le Fol, V., Ait-Aïssa, S., Sonavane, M., Porcher, J. M., Balaguer, P., Cravedi, J. P., Zalko, D., & Brion, F. (2017). In vitro and in vivo estrogenic activity of BPA, BPF and BPS in zebrafish-specific assays. *Ecotoxicology and Environmental Safety*, 142, 150–156. <https://doi.org/10.1016/j.ecoenv.2017.04.009>
- Lintelmann, J., Katayama, A., Kurihara, N., Shore, L., & Wenzel, A. (2003). Endocrine disruptors in the environment (IUPAC Technical Report). *Pure and Applied Chemistry*, 75(5), 631–681. <https://doi.org/10.1351/pac200375050631>
- Loos, R., Carvalho, R., António, D. C., Comero, S., Locoro, G., Tavazzi, S., Paracchini, B., Ghiani, M., Lettieri, T., Blaha, L., Jarosova, B., Voorspoels, S., Servaes, K., Haglund, P., Fick, J., Lindberg, R. H., Schwesig, D., & Gawlik, B. M. (2013). EU-wide monitoring survey on emerging polar organic contaminants in wastewater treatment plant effluents. *Water Research*, 47(17), 6475–6487. <https://doi.org/10.1016/j.watres.2013.08.024>
- Mehrabani-Zeinabad, M., Achari, G., & Langford, C. H. (2015). Advanced oxidative degradation of bisphenol A and bisphenol S. *Journal of Environmental Engineering and Science*, 10(4), 92–102. <https://doi.org/10.1680/jenes.15.00015>
- Mishra, D. K., Dolan, K. D., & Yang, L. (2011). Bootstrap confidence intervals for the kinetic parameters of degradation of anthocyanins in grape pomace. *Journal of Food Process Engineering*, 34(4), 1220–1233. <https://doi.org/10.1111/j.1745-4530.2009.00425.x>
- Mohapatra, D. P., Brar, S. K., Tyagi, R. D., & Surampalli, R. Y. (2011). Occurrence of bisphenol A in wastewater and wastewater sludge of CUQ treatment plant. *Journal of Xenobiotics*, 1(1), 3. <https://doi.org/10.4081/xeno.2011.e3>
- Montes, F., Valavala, S., & Haselbach, L. (2005). A New Test Method for Porosity Measurements of Portland Cement Pervious Concrete. *Journal of ASTM International*, 2(1), 12931. <https://doi.org/10.1520/JAI12931>
- Moreman, J., Lee, O., Trznadel, M., David, A., Kudoh, T., & Tyler, C. R. (2017). Acute Toxicity, Teratogenic, and Estrogenic Effects of Bisphenol A and Its Alternative Replacements Bisphenol S, Bisphenol F, and Bisphenol AF in Zebrafish Embryo-Larvae. *Environmental Science and Technology*, 51(21), 12796–12805. <https://doi.org/10.1021/acs.est.7b03283>
- Nafees, M., & Waseem, A. (2014). Organoclays as Sorbent Material for Phenolic Compounds: A Review. *CLEAN - Soil, Air, Water*, 42(11), 1500–1508. <https://doi.org/10.1002/clen.201300312>
- Ohtani, B., Prieto-Mahaney, O. O., Li, D., & Abe, R. (2010). What is Degussa (Evonik) P25? Crystalline composition analysis, reconstruction from isolated pure particles and photocatalytic activity test. *Journal of Photochemistry and Photobiology A: Chemistry*, 216(2–3), 179–182. <https://doi.org/10.1016/j.jphotochem.2010.07.024>
- Onundi, Y., Drake, B. A., Malecky, R. T., DeNardo, M. A., Mills, M. R., Kundu, S., Ryabov, A. D., Beach, E. S., Horwitz, C. P., Simonich, M. T., Truong, L., Tanguay, R. L., Wright, L. J., Singhal, N., & Collins, T. J. (2017). A multidisciplinary investigation of the technical and environmental performances of TAML/peroxide elimination of Bisphenol A compounds from water. *Green Chemistry*, 19(18), 4234–4262. <https://doi.org/10.1039/C7GC01415E>
- Poyatos, J. M., Muñio, M. M., Almericia, M. C., Torres, J. C., Hontoria, E., & Osorio, F. (2010). Advanced Oxidation Processes for Wastewater Treatment: State of the Art. *Water, Air, and Soil Pollution*, 205(1–4), 187–204. <https://doi.org/10.1007/s11270-009-0065-1>
- Radian, A., Carmeli, M., Zadaka-Amir, D., Nir, S., Wakshal, E., & Mishael, Y. G. (2011). Enhanced removal of humic acid from water by micelle-montmorillonite composites: Comparison to granulated activated carbon. *Applied Clay Science*, 54(3–4), 258–263. <https://doi.org/10.1016/j.clay.2011.09.008>
- Ramirez, J. H., Costa, C. A., Madeira, L. M., Mata, G., Vicente, M. A., Rojas-Cervantes, M. L., López-Peinado, A. J., & Martín-Aranda, R. M. (2007). Fenton-like oxidation of Orange II solutions using heterogeneous catalysts based on saponite clay. *Applied Catalysis B: Environmental*, 71(1–2), 44–56. <https://doi.org/10.1016/j.apcatb.2006.08.012>
- Rendel, P. M., & Rytwo, G. (2020a). The Effect of Electrolytes on the Photodegradation Kinetics of Caffeine. *Catalysts* 2020, 10(6), 644. <https://doi.org/10.3390/CATAL10060644>
- Rendel, P., & Rytwo, G. (2020b). Degradation kinetics of caffeine in water by UV/H<sub>2</sub>O<sub>2</sub> and UV/TiO<sub>2</sub>. *Desalination and Water Treatment*, 173, 231–242. <https://doi.org/10.5004/dwt.2020.24693>
- Research & Markets. (2018). *Global Bisphenol A Market Report 2018: Analysis 2013–2017 & Forecasts 2018–2023*. Research & Markets. <https://www.prnewswire.com/news-releases/global-bisphenol-a-market-report-2018-analysis-2013-2017%2D%2Ddforecasts-2018-2023-300757673.html>. Accessed 14 Jan 2022.
- Rioja, N., Zorita, S., & Peñas, F. J. (2016). Effect of water matrix on photocatalytic degradation and general kinetic modeling. *Applied Catalysis B: Environmental*, 180, 330–335. <https://doi.org/10.1016/J.APCATB.2015.06.038>
- Rytwo, G. (2018). Securing the future: Clay-based solutions for a comprehensive and sustainable potable water supply system. *Clays and Clay Minerals*, 66(4), 209–222. <https://doi.org/10.1346/CCMN.2018.064114>
- Rytwo, G., & Daskal, G. (2016). *A system for treatment of polluted effluents*. PCT/IL2015/050944, WO2016042558 A1 (Patent No. PCT/IL2015/050944, WO2016042558 A1). PCT/IL2015/050944, WO2016042558 A1.
- Rytwo, G., & Zelkind, A. L. (2022). Evaluation of kinetic pseudo-order in the photocatalytic degradation of ofloxacin. *Catalysts*, 12(1), 24. <https://doi.org/10.3390/catal12010024>
- Rytwo, G., Kohavi, Y., Botnick, I., & Gonen, Y. (2007). Use of CV- and TPP-montmorillonite for the removal of priority pollutants from water. *Applied Clay Science*, 36(1–3), 182–190. <https://doi.org/10.1016/j.clay.2006.04.016>
- Rytwo, G., Klein, T., Margalit, S., Mor, O., Naftaly, A., & Daskal, G. (2015). A continuous-flow device for photocatalytic degradation and full mineralization of priority pollutants in water. *Desalination and Water Treatment*, 57(35), 16424–16434. <https://doi.org/10.1080/19443994.2015.1077749>
- Salahinejad, A., Naderi, M., Attaran, A., Meuthen, D., Niyogi, S., & Chivers, D. P. (2020). Effects of chronic exposure to bisphenol-S on social behaviors in adult zebrafish: Disruption of the neuropeptide signaling pathways in the brain. *Environmental Pollution*, 262, 113992. <https://doi.org/10.1016/j.envpol.2020.113992>
- Samineni, K. (2017). *Adsorption of Bisphenol S from Water Using Natural Sorbents*. University of Dayton.
- Schneider, J., Matsuoka, M., Takeuchi, M., Zhang, J., Horiuchi, Y., Anpo, M., & Bahnemann, D. W. (2014). Understanding TiO<sub>2</sub> Photocatalysis: Mechanisms and Materials. *Chemical Reviews*, 114(19), 9919–9986. <https://doi.org/10.1021/cr5001892>
- Seachrist, D. D., Bonk, K. W., Ho, S.-M., Prins, G. S., Soto, A. M., & Keri, R. A. (2016). A review of the carcinogenic potential of bisphenol A. *Reproductive Toxicology*, 59, 167–182. <https://doi.org/10.1016/J.REPROTOX.2015.09.006>
- Semiat, R. (2000). Present and Future. *Water International*, 25(1), 54–65. <https://doi.org/10.1080/02508060008686797>
- Staples, C. A., Dorn, P. B., Klecka, G. M., O'Block, S. T., Branson, D. R., & Harris, L. R. (2000). Bisphenol A concentrations in receiving

- waters near US manufacturing and processing facilities. *Chemosphere*, 40(5), 521–525. [https://doi.org/10.1016/S0045-6535\(99\)00288-X](https://doi.org/10.1016/S0045-6535(99)00288-X)
- Thayer, K. A., Taylor, K. W., Garantzios, S., Schurman, S. H., Kissling, G. E., Hunt, D., Herbert, B., Church, R., Jankowich, R., Churchwell, M. I., Scheri, R. C., Birnbaum, L. S., & Bucher, J. R. (2016). Bisphenol A, Bisphenol S, and 4-Hydroxyphenyl 4-Isopropoxyphenylsulfone (BPSIP) in Urine and Blood of Cashiers. *Environmental Health Perspectives*, 124(4), 437–444. <https://doi.org/10.1289/ehp.1409427>
- Theng, B. K. G. K. G., Churchman, G. J. J., Gates, W. P. P., & Yuan, G. (2008). Organically Modified Clays for Pollutant Uptake and Environmental Protection. In: *Soil Mineral Microbe-Organic Interactions* (pp. 145–174). Springer. [https://doi.org/10.1007/978-3-540-77686-4\\_6](https://doi.org/10.1007/978-3-540-77686-4_6)
- Unuabonah, E. I., & Taubert, A. (2014). Clay–polymer nanocomposites (CPNs): Adsorbents of the future for water treatment. *Applied Clay Science*, 99, 83–92. <https://doi.org/10.1016/j.clay.2014.06.016>
- Vandenberg, L. N., Hauser, R., Marcus, M., Olea, N., & Welshons, W. V. (2007). Human exposure to bisphenol A (BPA). In: *Reproductive Toxicology* (Vol. 24, Issue 2, pp. 139–177). Reprod Toxicol. <https://doi.org/10.1016/j.reprotox.2007.07.010>
- Wirasnita, R., Mori, K., & Toyama, T. (2018). Effect of activated carbon on removal of four phenolic endocrine-disrupting compounds, bisphenol A, bisphenol F, bisphenol S, and 4-tert-butylphenol in constructed wetlands. *Chemosphere*, 210, 717–725. <https://doi.org/10.1016/j.chemosphere.2018.07.060>
- Yamazaki, E., Yamashita, N., Taniyasu, S., Lam, J., Lam, P. K. S., Moon, H. B., Jeong, Y., Kannan, P., Achyuthan, H., Munuswamy, N., & Kannan, K. (2015). Bisphenol A and other bisphenol analogues including BPS and BPF in surface water samples from Japan, China, Korea and India. *Ecotoxicology and Environmental Safety*, 122, 565–572. <https://doi.org/10.1016/j.ecoenv.2015.09.029>
- Yang, Q., Gao, M., Luo, Z., & Yang, S. (2016). Enhanced removal of bisphenol A from aqueous solution by organo-montmorillonites modified with novel Gemini pyridinium surfactants containing long alkyl chain. *Chemical Engineering Journal*, 285, 27–38. <https://doi.org/10.1016/J.CEJ.2015.09.114>

(Received 13 May 2021; Revised 9 December 2021; AE: J.-H. Choy)